Development 138, 5003-5013 (2011) doi:10.1242/dev.071522

Apical migration of nuclei during G2 is a prerequisite for all nuclear motion in zebrafish neuroepithelia

Louis Leung[1,*], Abigail V. Klopper[1,2,*], Stephan W. Grill[1,2], William A. Harris[3] and Caren Norden[1,‡]

SUMMARY

Nuclei in the proliferative pseudostratified epithelia of vastly different organisms exhibit a characteristic dynamics – the so-called interkinetic nuclear migration (IKNM). Although these movements are thought to be intimately tied to the cell cycle, little is known about the relationship between IKNM and distinct phases of the cell cycle and the role that this association plays in ensuring balanced proliferation and subsequent differentiation. Here, we perform a quantitative analysis of modes of nuclear migration during the cell cycle using a marker that enables the first unequivocal differentiation of all four phases in proliferating neuroepithelial cells in vivo. In zebrafish neuroepithelia, nuclei spend the majority of the cell cycle in S phase, less time in G1, with G2 and M being noticeably shorter still in comparison. Correlating cell cycle phases with nuclear movements shows that IKNM comprises rapid apical nuclear migration during G2 phase and stochastic nuclear motion during G1 and S phases. The rapid apical migration coincides with the onset of G2, during which we find basal actomyosin accumulation. Inhibiting the transition from G2 to M phase induces a complete stalling of nuclei, indicating that IKNM and cell cycle continuation cannot be uncoupled and that progression from G2 to M is a prerequisite for rapid apical migration. Taken together, these results suggest that IKNM involves an actomyosin-driven contraction of cytoplasm basal to the nucleus during G2, and that the stochastic nuclear movements observed in other phases arise passively due to apical migration in neighboring cells.

KEY WORDS: Cell cycle, Interkinetic nuclear migration, Pseudostratified epithelia, Quantitative analysis, Zebrafish

INTRODUCTION

Originally observed in neuroepithelia (Sauer, 1935), interkinetic nuclear migration (IKNM) has recently been detected in the non-neural epithelia of a variety of organisms including *Drosophila* and *Nematostella* (Meyer et al., 2011). The pseudostratified morphology of epithelia exhibiting IKNM has been implicated in maximizing the density of generative cells per unit area of apical surface over evolution (Fish et al., 2008). This suggests that IKNM is a ubiquitous feature of proliferating pseudostratified epithelia, and indicates that it plays a role in the faithful proliferation and development of multiple tissues. Despite a myriad of investigations into the molecular mechanics of nuclear movements during IKNM (Murciano et al., 2002; Baye and Link, 2007; Norden et al., 2009; Schenk et al., 2009; Tsai et al., 2010; Kosodo et al., 2011; Meyer et al., 2011), the exact extent to which nuclear movement influences development, and how the cell cycle influences IKNM, remain unclear.

In a pioneering study in the 1930s, prior to the development of live cell imaging techniques, IKNM was studied using fixed tissue analysis of developing neuroepithelia (Sauer, 1935). The working hypothesis resulting from this and other studies was that mitosis and cytokinesis take place at the apical side of the epithelium, after which nuclei exhibit a unidirectional transition towards the basal side of the cell during G1 and undergo S phase there, before migrating back towards the apical side during G2 (Kosodo et al., 2011; Miyata, 2008; Sauer, 1935). The idea that apical to basal movement might involve a passive component was raised in Sauer's original study. Indeed, a recent study using time-lapse imaging has shown that microbeads introduced into mouse neocortex move passively between cells towards the basal side in a unidirectional 'ratcheting' manner, most likely being displaced by apically migrating nuclei (Kosodo et al., 2011). This idea is corroborated by time-lapse studies in the zebrafish retina that show that there appear to be two kinds of nuclear movement. The first is rapid, persistently apically directed, actomyosin driven, and immediately precedes M phase. The second is slow, stochastic, happens throughout most of interphase, and is partially dependent on the first (Norden et al., 2009). These findings point towards a role for active nuclear migration in facilitating mitosis at the apical side of the epithelium via passive displacement of nuclei in cells at other points in the cell cycle. However, no study to date has been successful in distinguishing all cell cycle phases clearly during IKNM (Kosodo et al., 2011; Norden et al., 2009), a feat that would provide vital information about precisely when stochastic (passive) and directed (active) movements appear. Since other studies in mouse neocortex claim that basal movement in G1 is an active process mediated by microtubules and plus end-directed motors (Tsai et al., 2010), a detailed quantitative analysis of the phenomenon and its exact relationship with cell cycle events is essential for a full understanding of IKNM.

The key tool required for such an analysis is a marker that is capable of unambiguous detection of all four cell cycle phases. Here, we use fluorescently tagged proliferating cell nuclear antigen (PCNA), a DNA processivity factor for DNA polymerase without enzymatic activity. We track nuclei in each phase and analyze our measurements within a carefully formulated model for stochastic versus directed motion. This approach provides a precise picture of cell cycle phase length and its variability during tissue development

[1]Max Planck Institute of Molecular Cell Biology and Genetics, Pfotenhauerstraße 108, 01307 Dresden, Germany. [2]Max Planck Institute for the Physics of Complex Systems, Nöthnitzer Straße 38, 01187 Dresden, Germany. [3]Department of Physiology, Development and Neuroscience, University of Cambridge, Downing Street, Cambridge, CB2 3DY, UK.

*These authors contributed equally to this work
‡Author for correspondence (norden@mpi-cbg.de)

Accepted 15 September 2011

and thereby bears distinct advantages over phase length estimates derived from experiments on fixed tissue (Calegari and Huttner, 2003; Lange et al., 2009; Pilaz et al., 2009).

We can further understand the implications of stochastic and persistently directed nuclear movements by probing the relationship between IKNM and cell cycle progression. At present, the literature linking IKNM to the cell cycle is contradictory. Whereas S-phase arrest does not appear to affect nuclear migration in the chick diencephalon, implying that the cell cycle and IKNM are regulated by different machineries (Murciano et al., 2002), the inhibition of cell cycle progression induces an IKNM arrest in mouse telencephalon (Ueno et al., 2006). It should be noted, however, that these studies are based on BrdU pulse labeling in fixed tissue. A recent investigation showed that G1 arrest in slice cultures of rodent cortex leads to nuclear accumulation at basal positions in the epithelium and that S-phase arrest by hydroxyurea (HU) reveals a qualitative slow down of nuclear movement (Kosodo et al., 2011). However, no direct quantitative analysis of how cell cycle arrest at different stages influences nuclear movement in the whole epithelium has been performed. Furthermore, the way in which nuclear movement is affected by blocking entry into mitosis is as yet unknown.

We report here on the length and variability of different phases of the cell cycle in zebrafish retina and hindbrain neuroepithelia. We map modes of migration to these phases and examine how actomyosin accumulations change during the cell cycle. We unequivocally demonstrate that IKNM is directly coupled to cell cycle progression, as the directed apical movements during G2 drive the majority of all nuclear movements seen in other cell cycle phases.

MATERIALS AND METHODS

Animals

Zebrafish were maintained and bred at 28.5°C. Embryos were staged as previously described (Kimmel et al., 1995) in hours post-fertilization (hpf). Embryos were treated with 0.003% phenylthiourea (Sigma) to delay pigmentation.

Constructs

The PCNA-GFP vector was a gift from the Cardoso laboratory (Leonhardt et al., 2000). PCNA-GFP was subcloned into the pCS2+ vector using the *Xba*I and *Bam*HI sites. The MRLC:td:RFP construct in pCS2+ was a gift from the Paluch laboratory (MPI-CBG, Dresden). pCS2+ MRLC2^{T18DS19D} is published (Norden et al., 2009). RNA was synthesized using the SP6 mMessage Machine Kit (Ambion).

DNA/RNA injections

DNA injections (5 nl of 1 ng/μl) were performed at the one-cell stage, and RNA injections (5 nl of 100 ng/μl) at the 16- to 64-cell stage, to ensure a mosaic expression pattern of fluorophore-coupled constructs.

Drug treatments

Embryos mounted in 1% low melting point agarose and covered with embryo medium were used for experiments in which drugs were added at the beginning of a time-lapse experiment. RO-3306 (Enzo Life Science) was prepared as a 15 mM stock and used at 1 mM. HU (Sigma) was prepared as a 1 M stock and used at 40 mM. Aphidicolin (Sigma) was prepared as a 30 mM stock and used at 300 μM.

EdU injection

For EdU experiments (supplementary material Fig. S1), 50 μM EdU (Invitrogen; in 1% Phenol Red) injections were made into the third brain ventricle of anaesthetized 24 hpf embryos restrained in 1% low melting point agarose. Embryos were retrieved and fixed in ice-cold 4% paraformaldehyde in PBS. After brief washing, EdU was labeled with the Click-iT-Alexa 488 fluorophore kit (Invitrogen) according to the manufacturer's instructions and stored in PBS. *z*-stacks of retinas were taken on a Zeiss LSM 510 confocal microscope at 1 μm intervals and the center 2 μm were transformed into a maximal projection for nuclei counting using the Cell Counter plug-in in ImageJ (NIH).

Retinal lamination

For retinal lamination experiments (supplementary material Fig. S2C,D), *ptf1a;ath5* double transgenics were used. PCNA-GFP was injected and embryos were scanned live using a Zeiss LSM 510 confocal microscope with *z*-slice intervals of 1 μm.

In vivo imaging

Embryos were prepared for imaging as described (Zolessi et al., 2006). Fluorescence in the specimens was imaged using an UltraVIEW ERS spinning disk microscope (Perkin Elmer), an IX81 inverted microscope and a 60× water-immersion objective (Olympus), an Andor spinning disk microscope using IQ 1.10.3 acquisition software (Andor), or an LSM 510 confocal using an upright Axioplan 2 microscope and a 40× dipping objective (Zeiss) with Zeiss acquisition software. Samples were held at 30°C. Movies of the retina began between 26 and 28 hpf, and of the hindbrain between 22 and 24 hpf. These stages ensured that the vast majority of nuclei were still in the proliferative stage and featured very little, if any, neurogenesis. Optical sections 1 μm apart were taken through a volume of the retina and hindbrain up to 30 μm in depth. In the retina, movies were strictly taken in the central part of the retina away from the ciliary marginal zone and at a depth of the retina in which cellular angles do not obscure the analysis (Norden et al., 2009). Time points were 5 minutes apart, except for the PCNA-GFP/MRLC:td:RFP movies, where time points were 2 minutes apart. The 4D data obtained were processed and analyzed using Volocity (Improvision) or Fiji/ImageJ. Trajectories were obtained in Fiji/ImageJ software.

Statistical analysis of nuclear motion

Cell cycle phase-dependent instantaneous velocity distributions

One-dimensional nuclear trajectories were determined by projecting the displacement x of every nucleus in each frame onto the apicobasal axis. Displacements were measured relative to the point of contact with the basal lamina at 5-minute intervals in maximal projections that ensured that the whole length of the nucleus was captured (for details, see Norden et al., 2009). We transformed this time series into one of instantaneous velocity, defining the nuclear velocity in the jth frame as:

$$v(j\,\delta t) = \frac{x((j+1)\delta t) - x(j\,\delta t)}{\delta t} \quad ,$$

where δt denotes the time interval between frames. Positive (negative) values correspond to apical (basal) movements. Probability densities for instantaneous velocities were plotted and fitted as single and double Gaussian distributions.

MSD calculation

We used the mean squared displacement (MSD) as a function of elapsed time to characterize the type of motion involved in IKNM during different cell cycle phases. For each trajectory, the MSD was calculated as a function of elapsed time after n frames as:

$$MSD(\Delta t_n) \equiv MSD(n\,\delta t) = \frac{1}{N-n}\sum_{j=1}^{N-n}(x((j+n)\delta t) - x(j\,\delta t))^2 \quad ,$$

where N denotes the total number of 5-minute frames in a given movie and $n<N$ is a positive integer indexing 5-minute time lapses in Fig. 3A-C. We then averaged this quantity over all nuclear trajectories, for which N varied significantly, as shown in Fig. 1C,D. In wild type, N ranged from 10 to 43 in G1, from 17 to 135 in S, and from 4 to 20 in G2.

RESULTS

PCNA differentiates cell cycle phases in proliferative zebrafish neuroepithelia

In order to investigate the relationship between nuclear movement in neuroepithelia and particular phases of the cell cycle, we used a GFP-tagged version of PCNA to unambiguously differentiate

between the G1, S, G2 and M phases (Leonhardt et al., 2000). Although PCNA is a central component of the replication machinery, the absence of any known enzymatic activity of PCNA reduces the likelihood that slight overexpression of this construct interferes with cell cycle phase length. The original PCNA construct (Leonhardt et al., 2000) was subcloned into the CS2+ vector to permit mosaic expression through injection of mRNA into 16- to 64-cell stage zebrafish embryos. Visualizing PCNA in the zebrafish retina confirmed the localization pattern described previously (Leonhardt et al., 2000) (Fig. 1A and supplementary material Movie 1): even nuclear distribution in interphases G1 and G2, small dots covering the nucleus at the beginning of S phase, as well as larger accumulations late in S phase, and a diffuse cellular distribution in M phase upon nuclear envelope breakdown (Fig. 1A). This pattern makes PCNA an ideal marker for distinguishing between the G1, G2 and S phases during time-lapse imaging. It is also possible to detect M-phase entry and exit by the breakdown and reassembly of the nuclear envelope, respectively (Fig. 1A,B). The PCNA distribution pattern was similar in retinal and hindbrain neuroepithelia (Fig. 1A,B).

Defining cell cycle phase length and variability

Visualizing PCNA-GFP enabled the measurement of cell cycle phase lengths in intact neuroepithelia in vivo (Fig. 1C,D). The results are summarized in Table 1. For both retina and hindbrain, we found S phase to be the longest phase of the cell cycle. This

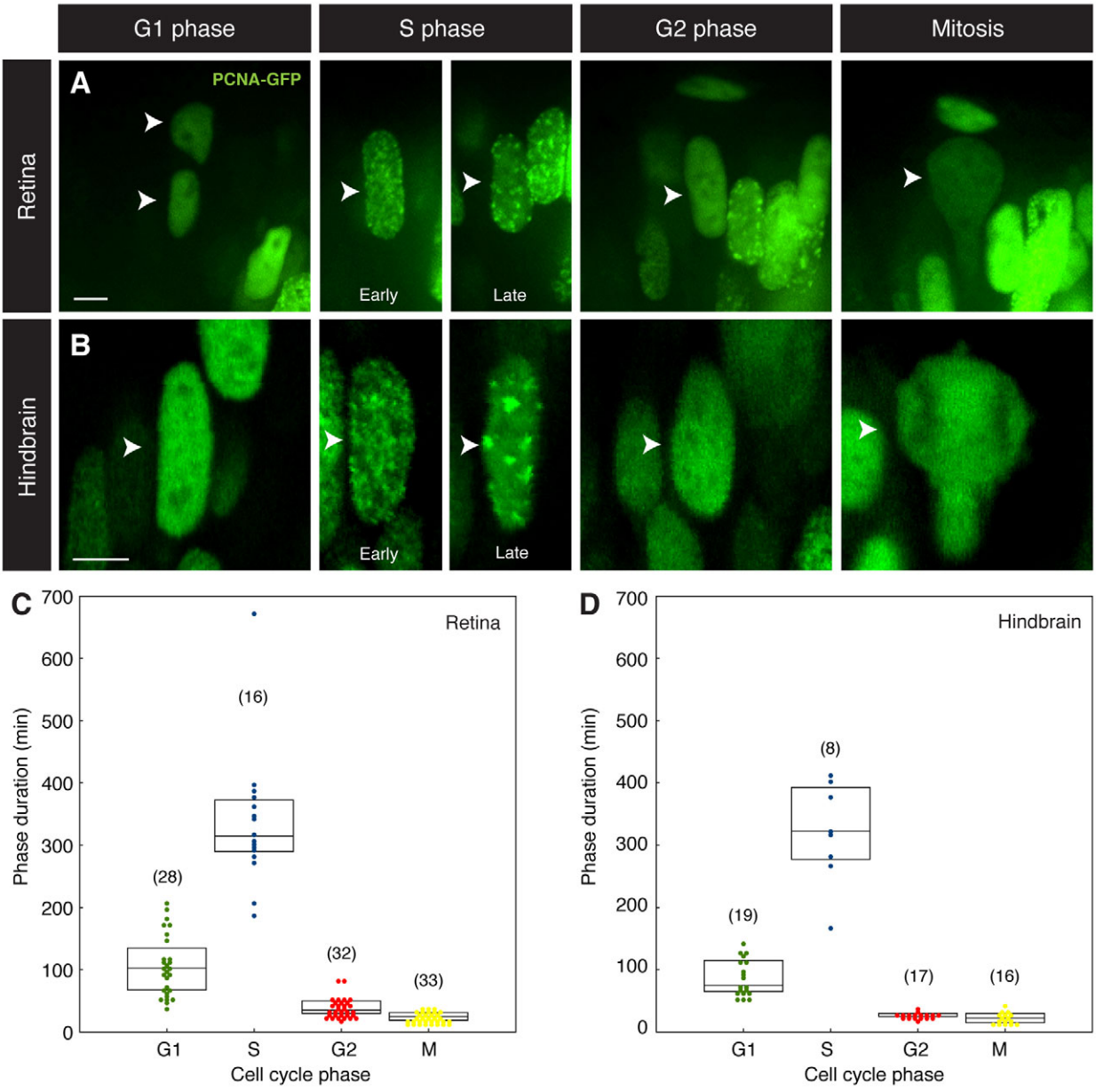

Fig. 1. PCNA-GFP marks cell cycle phases. (**A**) Still images of zebrafish retinal nuclei followed through the cell cycle. Phases can be identified by the differential distribution of PCNA-GFP (arrowheads). (**B**) Similar cell cycle phase identification is possible for nuclei in hindbrain neuroepithelia (arrowheads). (**C**,**D**) Box plots illustrating distributed lengths of cell cycle phases for retinal (C) and hindbrain (D) nuclei. The top and bottom of each box indicate upper and lower quartiles, respectively; the horizontal line represents the median. The number of nuclei followed for each cell cycle phase is indicated in parentheses. Scale bars: 10 μm.

Table 1. Phase periods for G1, S, G2 and M in retina and hindbrain

	G1	S	G2	M
Retina				
Phase length	108±19	337±57	40±6	25±3
COV	0.45	0.32	0.39	0.34
Hindbrain				
Phase length	89±14	321±66	29±2	24±5
COV	0.28	0.18	0.23	0.24

Mean and standard error of the mean of phase length are reported in minutes along with the coefficient of variation (COV: the ratio of standard deviation to mean).

finding is contrary to the assumption, based on fixed-tissue BrdU analyses, that in neural progenitors nuclei spend the majority of the cell cycle in G1 (Takahashi et al., 1995). However, it is consistent with the fact that, in both zebrafish and mouse retinas, a short BrdU pulse labels a large number of nuclei along the whole length of the epithelium (Baye and Link, 2007). We further validated our own observations by EdU labeling. With a short pulse of EdU at 28 hpf (30 minutes), we found that 62.7% of nuclei were in S phase, which is consistent with our finding that ~60% of the cell cycle is taken up by S phase at this stage (supplementary material Fig. S1F). Therefore, EdU faithfully corroborates the findings derived from following individual nuclei over time using PCNA-GFP.

Although there was variability in the duration of both the S and G1 phases between cells, we did not see any correlation between the lengths of G1 and S (R^2=0.004; supplementary material Fig. S3F), suggesting that the length of G1 does not influence the length of S phase. In comparison to S and G1, the G2 and M phases, which are also variable in length, are relatively short. Although the phase lengths of S and G1 have much broader distributions than those of G2 and M, the coefficient of variation (ratio of standard deviation to mean) is relatively similar in all four phases in both retina and hindbrain (see Table 1). Experiments with a PCNA-GFP DNA construct yielded similar phase length data (supplementary material Fig. S2B), indicating that moderate RNA overexpression did not influence the results. To additionally verify that embryonic development and retinal lamination were not impaired by the slight PCNA overexpression, we used transgenic embryos expressing *ptf1a*::dsRed (which labels amacrine and horizontal cells) and *ath5*::RFP (which labels retinal ganglion cells and a subset of photoreceptors; *ath5* is also known as *atoh7* – Zebrafish Information Network). We observed no differences in lamination or development between 56 hpf embryos that were injected with PCNA-GFP RNA at the 16-cell stage and 56 hpf uninjected control embryos (supplementary material Fig. S2D).

In conclusion, cell cycle phase lengths are comparable in neuroepithelia of different regions of the developing zebrafish brain. We show that proliferating neuroepithelial cells spend ~60% of the cell cycle in S phase, ~20% in G1 and ~10% in each of G2 and M. These data additionally clarify that the variability of cell cycle length reported elsewhere (Baye and Link, 2007) arises mainly from differences in the duration of the S and G1 phases.

Linking cell cycle phases to modes of movement during IKNM

Using the PCNA construct, we were able to characterize the nature of IKNM in different cell cycle phases by following nuclear trajectories in retina and hindbrain (Fig. 2A). Typical nuclear trajectories for retina and hindbrain are shown in Fig. 2B. These plots illustrate that IKNM displays similar characteristics in both epithelia. Plotting the displacements of each trajectory according to cell cycle stage clarifies the qualitative distinction between the different stages of the cell cycle in terms of nuclear movement (Fig. 2C).

In S phase, nuclei move in both directions without basal or apical bias. The positions at which nuclei undergo DNA replication in S are broadly distributed across the center of the epithelium (Baye and Link, 2007) (supplementary material Fig. S3A-D). It is therefore not surprising that the apicobasal position at which cells make the transition from S into G2 also ranges over the whole axis (supplementary material Fig. S3E). In contrast to nuclei in S phase, nuclei in G2 move with striking directionality. In both retina and hindbrain, the transition to G2 marks an immediate, persistent and rapid movement of nuclei towards the apical surface (supplementary material Movies 1 and 2). We note that velocities appear to be higher in the hindbrain than in the retina. Apical migration stops when the soma of the neuroepithelial cells rounds up at the apical surface, which coincides with the beginning of M phase.

There are two mechanisms by which nuclei may move towards the basal side of the epithelium during G1. They could use a directed process involving cytoskeletal components and motor proteins (Tsai et al., 2010) or there is a passive migration of nuclei displaced by incoming mitotic nuclei at the apical side (Sauer, 1935; Norden et al., 2009; Kosodo et al., 2011). Although a recent study in mouse cortex shows that incorporated microbeads can be passively displaced by incoming mitotic nuclei (Kosodo et al., 2011), a direct quantitative measurement of how nuclei move in G1 is yet to be performed. We used the PCNA marker to carry out such an analysis in live zebrafish neuroepithelia. If nuclear movements in G1 are mainly a secondary event to make room for incoming nuclei that are ready to divide, nuclear movements in G1 should be largely stochastic and similar to those observed during S phase, with the proviso that there is bound to be a basal drift to the displacement due to the fact that the apical surface forms a boundary to further movement in this direction. If there is a mechanism in place for active migration away from the apical surface, then movements in G1 should be highly directed like those in G2. As depicted in Fig. 2C, our results show that nuclear migration during G1 is largely stochastic, with a slight basal drift. We find no evidence for persistent unidirectional movement during this stage.

To achieve a complete understanding of the modes of motion observed during different cell cycle phases we supplemented this qualitative observation by invoking the principles and measures of stochastic processes. We study the mean square displacement (MSD) of nuclear trajectories as a function of elapsed imaging time. For particles subject to simple diffusion, the MSD is a linear function of elapsed time with a slope of 2*D*, where *D* is the one-dimensional diffusion coefficient. When the diffusion of the nuclei is restricted due to the proximity of a laminar surface that acts as a reflecting boundary, then the case is more complicated, and the MSD depends on the length of time for which one samples the trajectory. One can describe this behavior in terms of an effective drift velocity, similar to the case of nuclei undergoing directed motion as well as diffusion. Therefore, for both G1 and G2, the MSD displays a quadratic dependence on elapsed time and the slope of the quadratic function at the origin is 2*D* (Kusumi et al., 1993; Berg, 1993).

We summarize the results of our MSD analysis in Table 2. In S phase, we observe that the MSD of nuclei increases linearly with elapsed time for both retinal and hindbrain epithelia, meaning that nuclei diffuse randomly without any directionality (Fig. 3A-C).

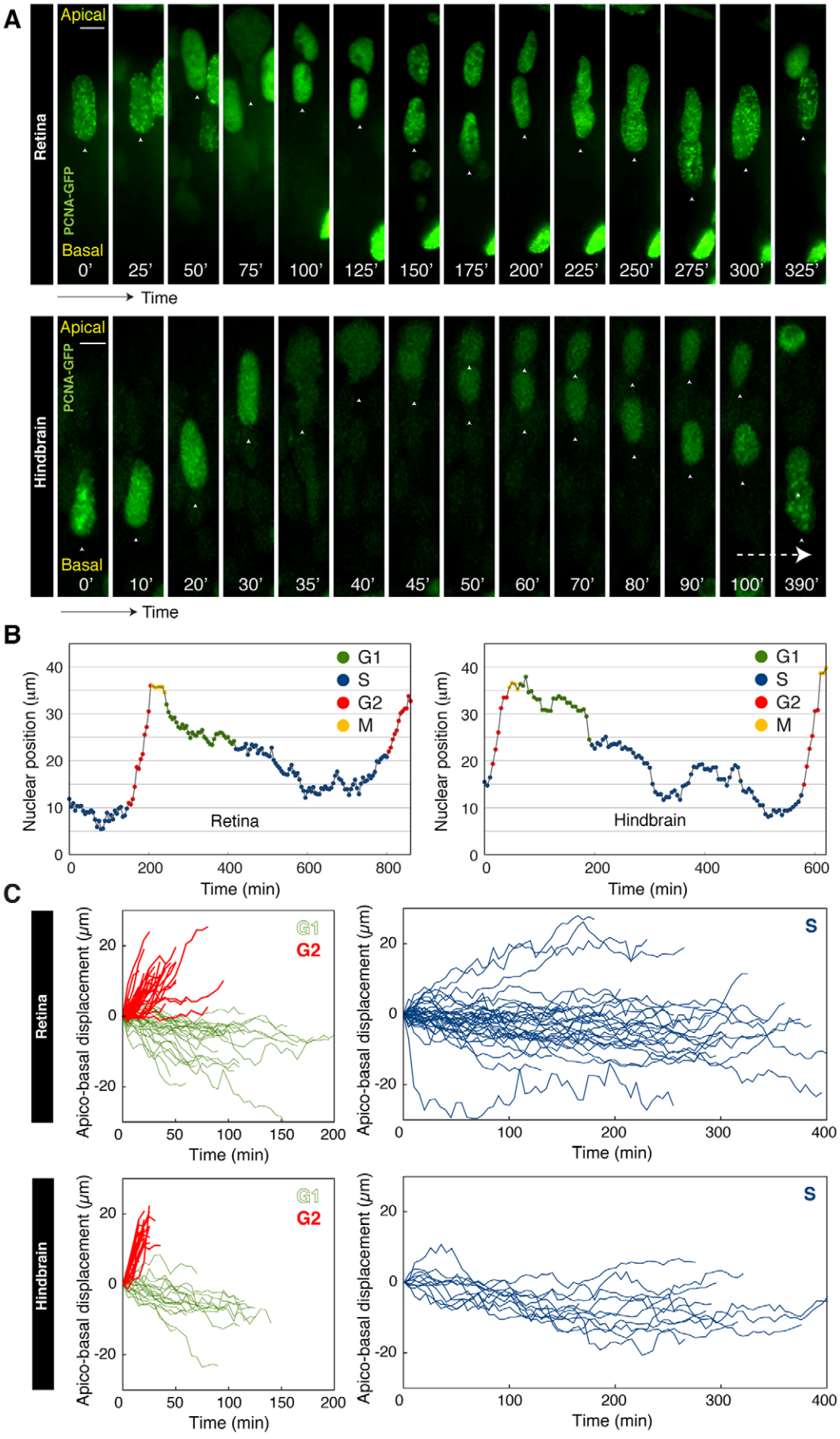

Fig. 2. Modes of nuclear migration tied to specific cell cycle phases. (**A**) Time-lapse imaging of zebrafish retinal/hindbrain nuclei expressing PCNA-GFP. Nuclei show stochastic movements in S and G1 with rapid directed apical motion in G2 phase followed by mitosis. (**B**) Typical trajectory of a retinal/hindbrain nucleus over time. (**C**) Displacement of nuclei in G1, G2 or S phase measured relative to the initial position at the start of each phase for retinal or hindbrain nuclei. Scale bars: 5 μm.

Table 2. Diffusion coefficients and drift velocities for G1, S, G2 and M phases in retina and hindbrain

	G1	S	G2
Retina			
D	0.192±0.004	0.210±0.001	0.42±0.05
μ	0.104±0.003	–	0.28±0.01
Hindbrain			
D	0.21±0.02	0.156±0.003	1.3±0.3
μ	0.07±0.02	–	0.63±0.03

Mean and standard error of the mean of the diffusion coefficient (*D*, μm²/minute) and drift velocity (μ, μm/minute) are reported.

During G1, the diffusion coefficients are very similar to those measured during S phase, and the MSD is best described as a quadratic function of elapsed time in both retina and hindbrain, with slight, but non-zero, effective drift velocities (Fig. 3A, detail in 3B). Importantly, this non-zero drift all but vanishes when we average over only the latter half of each nuclear trajectory during G1 (Fig. 3C), indicating that, as the nuclei drift basally, the effect of the apical surface boundary becomes negligible. This provides further evidence to suggest that movement in G1 is of a passive nature and stochastic rather than unidirectional. During G2, the drift is more pronounced, and the diffusion coefficients in both epithelia differ significantly from those measured during S and G1 (Fig. 3A). We expect to see this discrepancy resolved by finer time resolution, with which one can obtain a more accurate estimate of the slope and thus the diffusion coefficient. In all phases for both epithelia, coefficients from polynomial fits of higher order than those quoted here did not differ significantly from zero. These results clearly demonstrate that nuclear motion during G2 is strongly directed towards the apical side, in contrast to movement during the S (which is purely diffusive) and G1 (which involves stochastic motion beginning with a slow basal drift) phases.

Additionally, instantaneous velocity distributions were collated and evaluated for cell cycle stage-dependent analysis in both hindbrain and retina. All results are summarized in Table 3. As expected, distributions in S phase are well described by a Gaussian distribution with a mean of zero (Fig. 3D). This confirms that nuclear movement in S phase has no underlying directionality. As there was no differentiation between phases in a previous quantitative analysis of nuclear behavior in IKNM (Norden et al., 2009), one might postulate that a shifting average towards the basal side in G1 was masked by an oversampling of S, the longest phase in the cycle. However, G1 velocity distributions imply that this is not the case as they are well described by a Gaussian distribution centered near the origin, with a very slight basal drift in retina and hindbrain (Fig. 3D). By contrast, the distribution for G2 features a clear tendency towards apical velocities (Fig. 3D), suggesting that in G2 the nucleus moves towards the apical side of the epithelium before entering M phase (Fig. 3D). The distribution fits with a sum of Gaussian functions, showing that when nuclei in G2 are not migrating persistently in an apical fashion they are largely motionless. The analysis confirms our impression that G2 velocities in the hindbrain are higher than those in the retina.

These data suggest that G2 is the only phase of the cell cycle that can be linked to persistent directed movements. This movement is always directed towards the apical side. Although there seems to be a basal drift at the beginning of G1, this is much weaker than the apical movement in G2, and in S phase nuclear movement is completely stochastic.

Myosin is recruited to the basal side of the nucleus upon onset of G2 phase

Previous studies have shown that actomyosin contractions play a major role in IKNM, particularly during fast apical migration (Meyer et al., 2011; Norden et al., 2009). Having shown that rapid apical migration occurs exclusively during G2 phase, we set out to determine whether entry into G2 is the point at which the actomyosin cytoskeleton becomes activated to induce apical migration of nuclei. To investigate if, and how, entry into G2 correlates with changes in actomyosin activity and localization, we performed time-lapse experiments using fluorescently tagged myosin together with PCNA-GFP. We used a Myosin regulatory light chain (MRLC:td:RFP) construct to visualize the distribution of the activator of Myosin II contractility (supplementary material Movies 5 and 6). This is a better marker than the constitutively active version of MRLC (Norden et al., 2009) as it allows for a more accurate analysis of myosin distributions and their changes.

We found that in G1 and S phases, nuclei are surrounded by MRLC symmetrically (Fig. 4A and supplementary material Movie 5). In striking contrast to this, a basal accumulation of MRLC (and thus a break of the actin symmetry observed in G1 and S) coincides temporally with the transition of nuclei into G2 phase, appearing 5-10 minutes after the prominent S-phase PCNA dots disappear (arrowhead Fig. 4B; supplementary material Movie 6). This basal accumulation seems to guide the nucleus towards the apical side. Once the nucleus reaches an apical position, the myosin forms a basal concentration, which constricts the cleavage furrow (supplementary material Movie 6, arrowhead). The temporal correlation between the basal localization of MRLC and G2 onset suggests that the S/G2 transition prompts asymmetric basal actomyosin activation, which squeezes nuclei towards the apical side of the neuroepithelium as the cell cortex constricts basal to the nucleus. This confirms earlier results suggesting that actomyosin activity and rapid apical migration are linked (Norden et al., 2009) and shows that this is coupled to actomyosin redistribution towards the basal side of the nucleus.

Cell cycle continuation is a prerequisite for fast, persistent apical migration

The dependence of IKNM on the progression of the cell cycle has become a focal point of investigation in recent years (Murciano et al., 2002; Ueno et al., 2006; Kosodo et al., 2011). However, the effect of cell cycle arrest on IKNM at an epithelial level is yet to be quantitatively characterized. We performed a quantitative analysis of experiments carried out to obtain additional kinetic information in order to understand how blocking the cell cycle at particular phases affects IKNM. To arrest nuclei in S phase, we used a mixture of Aphidicolin and HU, which has been shown to lead to more stringent blockage than HU alone (Menozzi et al., 1985; Harris and Hartenstein, 1991). Drugs were added at the beginning of the time-lapse experiment and after 2 hours nuclei were still able to enter S phase but did not progress further in the

Table 3. Instantaneous velocity for G1, S, G2 and M in retina and hindbrain

	G1	S	G2
Retina	–0.08±0.01	0.00±0.01	0.30±0.02
Hindbrain	–0.09±0.02	–0.01±0.01	0.62±0.06

Mean and standard error of the mean are reported for instantaneous velocity (μm/minute).

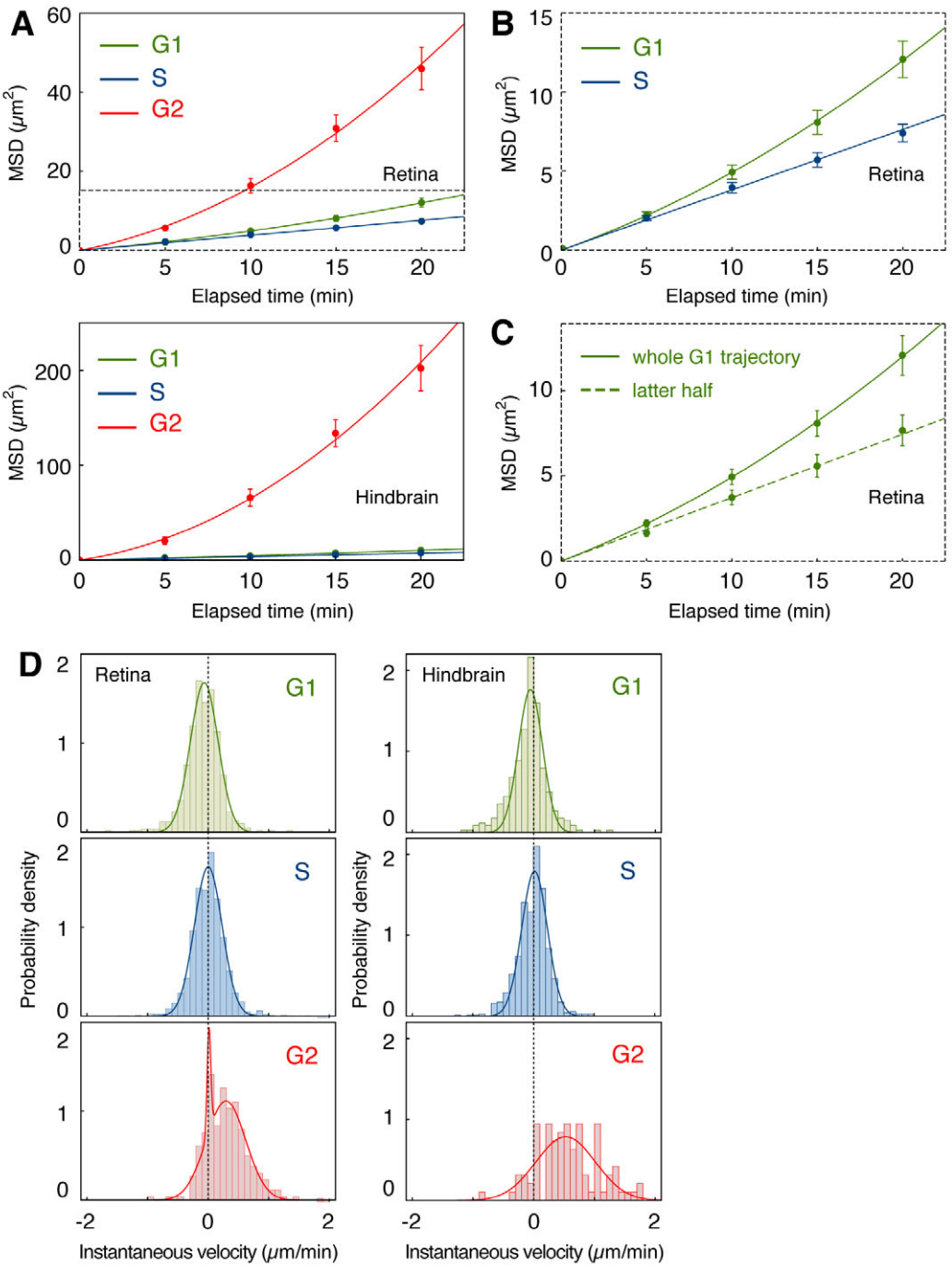

Fig. 3. Quantitative analysis of nuclear motion in retina and hindbrain epithelia. (**A**) Mean squared displacement (MSD) of zebrafish retina (top) and hindbrain (bottom) nuclei as a function of elapsed time for G1, S and G2 nuclei. In both epithelia, quadratic dependence of the MSD on elapsed time indicates that motion during G2 is clearly directed. (**B**) A magnification (boxed area in A) of the MSD for G1 and S in the retina. (**C**) Averaging MSD over the latter half of each G1 trajectory (dashed line) demonstrates that the basally directed motion is restricted to the start of G1. Note that solid green lines in A (top), B and C are identical. Error bars indicate s.e.m. (**D**) Instantaneous velocity distributions (bars) and Gaussian fit (bold line) for retinal/hindbrain data grouped into cell cycle phases. The distribution for G2 in the retina fits with a sum of Gaussians, demonstrating the bimodality of motion here.

cell cycle (Fig. 5A and supplementary material Movie 3). The persistence of nuclear dots once cells are blocked in S phase is also further verification that PCNA labels cell cycle phases correctly in developing zebrafish neuroepithelia. More importantly, however, this blockade coincided with the absence of any rapid and persistent apically directed motion of the type normally seen in G2 (Fig. 5A and supplementary material Fig. S4A and Movie 3). For the nuclei arrested in S phase, both velocity distributions and MSD versus elapsed time suggest that movement is reduced compared with wild-type S phase (Fig. 5C). The results are similar to those obtained by Myosin II blockade (Norden et al., 2009) and indicate that the random movements observed in S phase are strongly

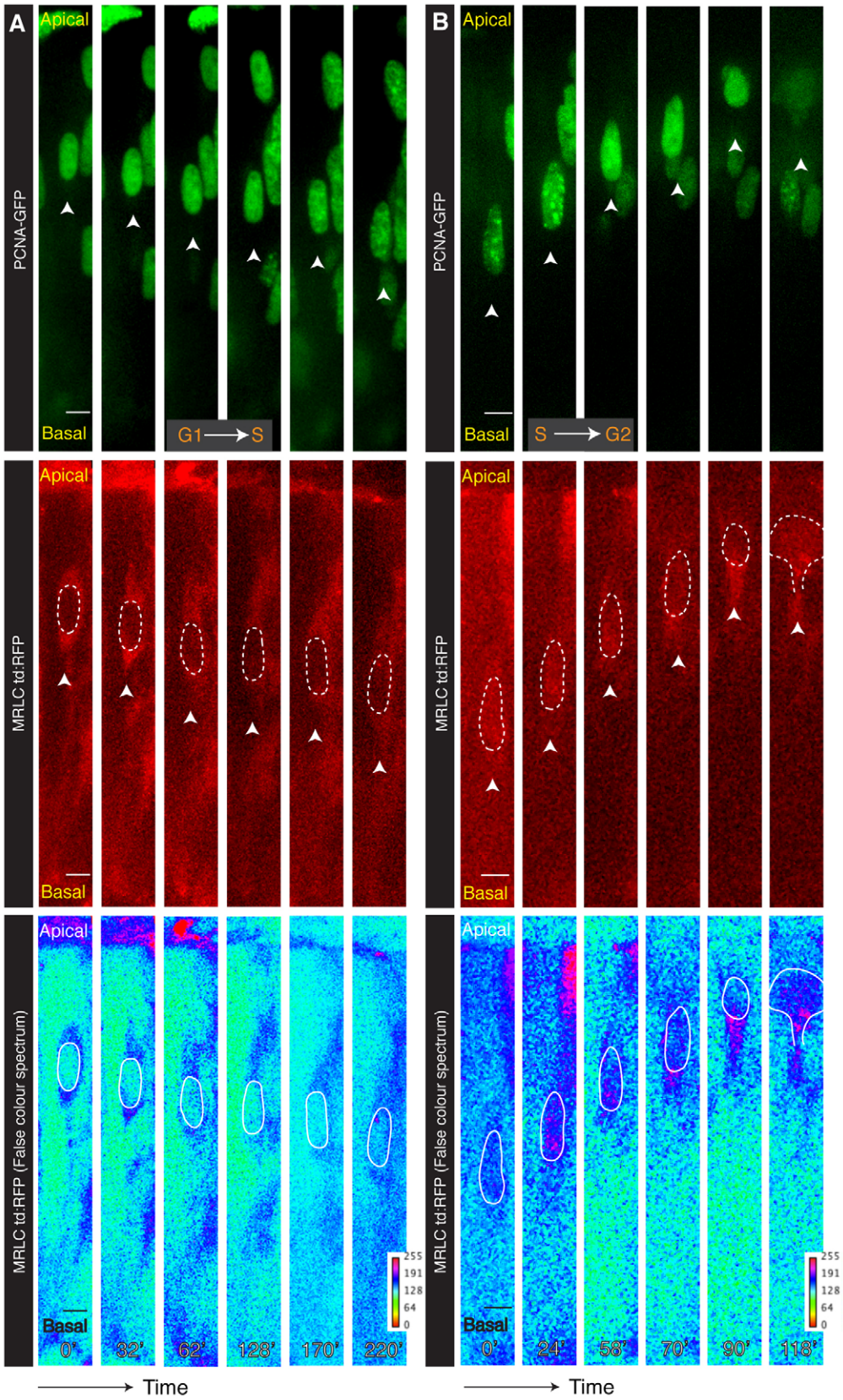

Fig. 4. Temporal relationship of myosin localization with specific cell cycle phases. (**A**) Kymograph from supplementary material Movie 5 showing that Myosin regulatory light chain (MRLC) surrounds nuclei symmetrically in G1 and S phases. (**B**) Kymograph from supplementary material Movie 6 showing that MRLC accumulates basally after nuclei have entered G2 and separately for the cytokinetic furrow. The nucleus traced using the PCNA-GFP channel is outlined with broken line. Arrowheads in PCNA-GFP and MRLC:td:RFP channels are in equivalent positions, indicating the basal side of the nucleus over time. Scale bars: 5 μm.

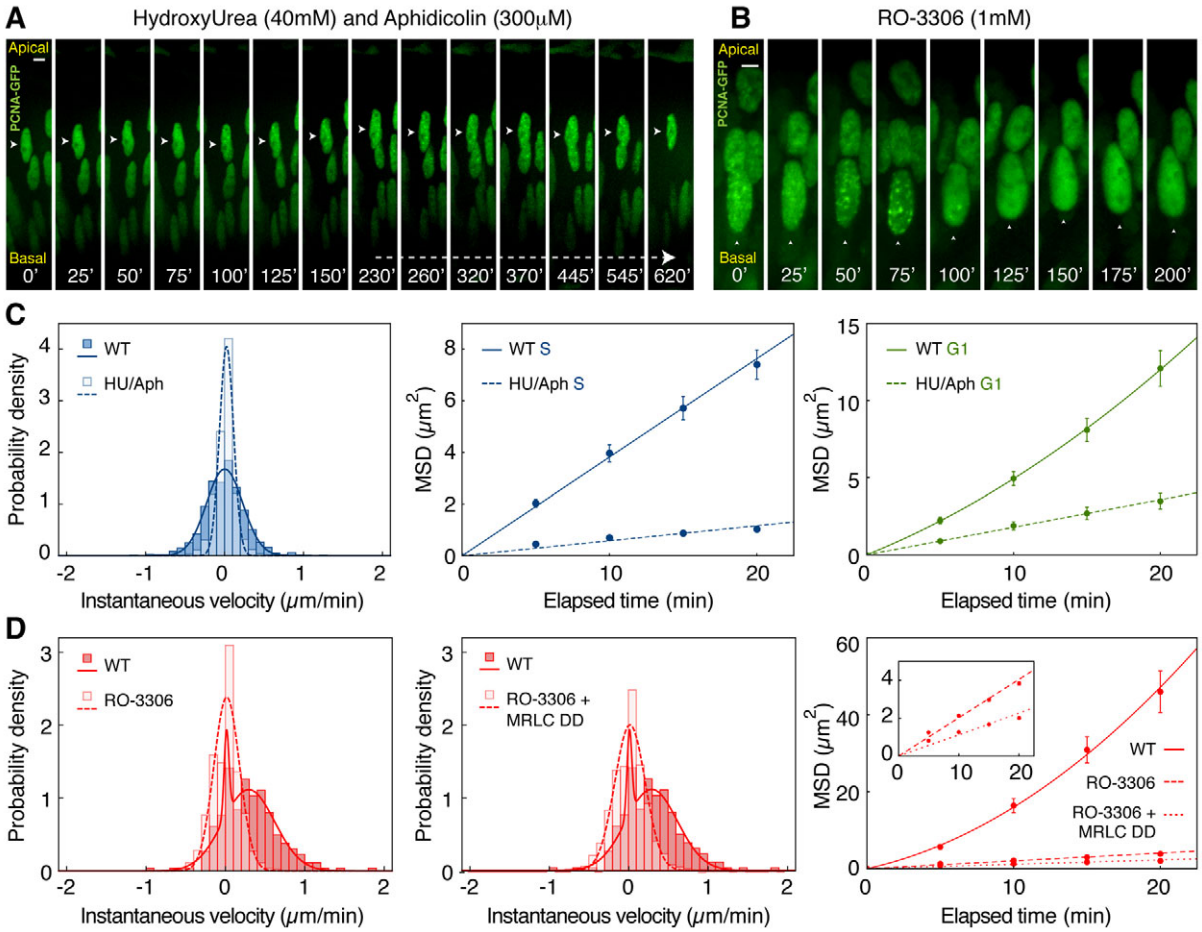

Fig. 5. Cell cycle continuation is required for directed nuclear motion. Time-lapse imaging of nuclei blocked with pharmacological inhibitors of specific cell cycle phases. (**A**) Kymograph of retinal nucleus (arrowhead) in the presence of the S/G2 inhibitors HU and Aphidicolin, entering but remaining in S phase. (**B**) Kymograph of a retinal nucleus (arrowhead) in the presence of the G2/M inhibitor RO-3306, entering G2 but not migrating towards the apical surface. (**C**) Velocity distribution and MSD analysis confirm the absence of directed motion during S phase and a marked reduction in the effective displacement of treated nuclei. The MSD during G1 in treated zebrafish embryos increases linearly with elapsed time, in contrast to wild-type nuclei. (**D**) Velocity distribution and MSD analysis show the absence of directed motion in RO-3306-treated embryos. This effect cannot be rescued by co-expression of constitutively active Myosin regulatory light chain (MRLC-DD). Error bars indicate s.e.m. Scale bars: 5 μm.

reduced when cells are prevented from entering G2. Similarly, the behavior of MSD with time indicates that treatment with HU and Aphidicolin blocks basal drift in G1 (Fig. 5C). This in turn suggests that the majority of the stochastic movements of nuclei in other phases of the cell cycle are passive consequences of nuclei moving rapidly to the apical surface during G2.

Cdk1 activity is required for entry and progression through mitosis and in its absence cells are unable to undergo the G2/M transition (Vassilev et al., 2006). In order to elaborate on the above findings with a drug that arrests cells in G2 and thereby prevents this transition, we added the small compound RO-3306, which has been shown to reversibly inhibit Cdk1 activity (Vassilev et al., 2006), at the beginning of time-lapse experiments of PCNA-GFP-injected fish (supplementary material Movie 4). As expected, we observed a disappearance of the typical dotted PCNA distribution, indicating exit from S phase. However, in RO-3306-treated embryos, exit from S phase was not followed by the apical translocation of nuclei, but instead nuclei remained at their respective positions (Fig. 5B and supplementary material Movie 4 and Fig. S4B). To analyze this behavior quantitatively, we repeated the experiment adding the drug 5 hours before the time-lapse. At the start of imaging, most nuclei were arrested. These nuclei were followed over time and trajectories were generated. Both velocity distributions and MSD time dependence differ markedly from the wild-type situation (Fig. 5D). Velocity distributions are centered around zero and no positive drift can be observed. The MSD increases linearly with elapsed time and the diffusion coefficient (0.057±0.004 μm^2/minute) is substantially smaller than that of wild-type nuclei.

Since RO-3306 acts as a Cdk1 inhibitor, one might ask whether the stalling of nuclei is a result of the cell cycle arrest or is a direct effect of perturbing the cytoskeleton. Nuclear stalling by Myosin II inhibition can be partly rescued by overexpression of a constitutively active Myosin II construct (MRLC2^{T18DS19D}) (Norden et al., 2009). Therefore, to test whether the RO-3306 inhibition is linked to actomyosin inhibition rather than to the cell cycle, MRLC2^{T18DS19D} RNA was injected into one-cell stage embryos, and PCNA was injected at the 16- to 64-cell stage to ensure mosaic expression. As before, RO-3306 was added 5 hours before the start of the time-lapse experiment and trajectories were analyzed. Velocity distributions and MSD elapsed time dependence

show no rescue effect under these conditions (Fig. 5D). Velocities are normally distributed around zero. The diffusion coefficient remains significantly reduced (0.101±0.004 μm^2/minute) and the MSD increases linearly with elapsed time. Interestingly, there is a slight broadening of the velocity distributions and a larger diffusion coefficient than that observed in the RO-3306 experiments. This suggests that the expression of constitutively active Myosin II can induce random cortical contractions, which are able to move nuclei in an undirected manner.

Our data demonstrate that the transition to G2 and the concomitant activity of Cdk1 are prerequisites for the apical migration of nuclei before mitosis. They also indicate that such directed movements occur only during G2, and that these drive the stochastic motion of nuclei in the other phases of the cell cycle.

DISCUSSION

Using PCNA-GFP we have investigated the complex interdependence of IKNM and the cell cycle in proliferative neuroepithelial cells of the zebrafish. We measured the time that nuclei spend in each of the four phases of the cell cycle. We found that, on average, S is the longest phase of the cycle in both zebrafish retina and hindbrain, being approximately three times longer than G1, which is itself much longer than the G2 and M phases. G1 and S phase lengths are characterized by broader distributions than those of G2 and M, but all phases share similar coefficients of variation despite their different average values. This relationship, coupled with the lack of correlation between the lengths of G1 and S within single cells (supplementary material Fig. S3F), suggests that cell cycle phase lengths are independently and loosely regulated by mechanisms that give rise to similar statistics in these neuroepithelial cells.

Our data characterize the nature of IKNM in distinct cell cycle phases for the first time in vivo in a quantitative manner. We found that nuclei undergo stochastic motion during both G1 and S, resulting in a very broad distribution of nuclear positions in the apicobasal domain at the onset of G2. This differs markedly from mammalian neocortex, in which S-phase nuclei predominantly occupy very basal positions. Following S phase, nuclei are driven in a persistent and highly directed fashion towards the apical surface where they immediately enter M phase. This migration constitutes the only persistent motion in the entire cell cycle. The movements coincide with asymmetric myosin accumulation on the basal side of the nucleus upon the transition from S to G2, suggesting that the nucleus is being squeezed towards the apical side by constriction of the basal cortex and thereby the cytoplasm. A non-zero basal drift velocity in G1 is observed for nuclei exiting M phase. We cannot exclude the possibility that an active mechanism might push the spindle away from the apical side during mitosis or very early in G1. However, in the latter half of G1, nuclear movement is clearly stochastic and bidirectional. This, combined with the fact that the basal drift early in G1 vanishes upon the introduction of drugs that prevent the apical migration in G2 (Fig. 5C), strongly suggests that the simplest explanation for our results is that, in short neuroepithelia like the zebrafish hindbrain and retina, nuclear displacement towards the basal side in G1 is largely a passive process. Nevertheless, more thorough studies are needed to validate this point, ideally using a 3D approach that takes into account all nuclei in the tissue. Furthermore, we certainly cannot exclude the possibility that more active forces facilitate basal displacement in more elongated neuroepithelia such as the rodent cortex (Tsai et al., 2010), although indirect studies suggest otherwise (Kosodo et al., 2011).

Investigations of the interdependence of the cell cycle and IKNM have yielded contradictory reports to date (Murciano et al., 2002; Ueno et al., 2006). A recent live imaging study using HU to block S-phase exit in mouse neocortex reported a slow down, but not cessation, of nuclear movement (Kosodo et al., 2011). Using HU in combination with Aphidicolin to generate stringent S-phase blocking, we show that all nuclear movements grind to a halt upon inhibition of S phase. Careful statistical analysis indicates that stochastic movements still occur but are far less pronounced than those in the wild type. We further show that nuclei blocked at the G2/M transition via Cdk1 inhibition do not undergo fast apical migration. This implies that completion of S phase is not sufficient to trigger apical translocation, but that a Cdk1-dependent process in G2 leading to progression through M phase is required. Developing an understanding of how cell cycle phase, cyclin-dependent signaling and actomyosin contractility are linked forms a challenging task for the future. Inhibiting the cell cycle in S phase or blocking Cdk1 activity prohibits not only persistent apical migration but also minimizes the stochastic movements observed in G1 and S. This corroborates our claim that nuclei do not actively migrate away from the apical surface during G1 but are rather jostled out of the way as cells in G2 drive their nuclei apically.

The fact that the nuclear movements we observed do not significantly differ between retinal and hindbrain neuroepithelia supports the notion that the conclusions we draw here and elsewhere (Norden et al., 2009) hold in all zebrafish neuroepithelia. Future comparison of these findings with those in other epithelia characterized by IKNM will prove enlightening. An important example is the significantly longer neuroepithelium of the rodent cortex. As mentioned above, the zebrafish retina and hindbrain are evolutionarily older than the mammalian cortex. One could therefore hypothesize that IKNM in these neuroepithelia serves the sole purpose of maximizing generative density by randomly displacing nuclei that are not undergoing mitosis. In these relatively short neuroepithelia, actomyosin contractile mechanisms appear sufficient to translocate nuclei towards the apical side of the epithelium before mitosis. Further support for this notion comes from the fact that IKNM in other short and evolutionarily older epithelia, such as the *Drosophila* wing disc and *Nematostella* ectoderm (Meyer et al., 2011), depend on actomyosin contractions. It might well be, however, that during the evolution of the mammalian cortical neuroepithelium, the extreme elongation of the neuroepithelium and the denser packing of nuclei may have compromised the ability of actomyosin to drive nuclei towards the apical side. In this context, microtubules seem to play a more important role (Tsai et al., 2010; Kosodo et al., 2011). Probing the differences between IKNM in different epithelia will lend important insight into the cell biological and evolutionary aspects of nuclear migration in elongated epithelia and how they influence the proliferation and development of tissue. In this respect, combining PCNA with live imaging methods represents an exciting new tool that also has the potential to be used for cell cycle phase-dependent analyses in other contexts, particularly to substantiate results obtained using fixed tissue and BrdU staining.

Acknowledgements

We thank J. Pines and J. Mansfeld for inspiring discussions and sharing the PCNA-GFP construct; E. Paluch for sharing the MRLC:td:RFP construct; F. Calegari for advice on EdU experiments; J. Huisken for input on data presentation; and S. R. Young for discussion and helpful comments on the manuscript.

Funding
L.L., A.V.K., S.W.G. and C.N. are funded by the Max Planck Society. W.A.H. holds a Wellcome Trust Programme Grant. Deposited in PMC for release after 6 months.

Competing interests statement
The authors declare no competing financial interests.

Supplementary material
Supplementary material available online at
http://dev.biologists.org/lookup/suppl/doi:10.1242/dev.071522/-/DC1

References
Baye, L. M. and Link, B. A. (2007). Interkinetic nuclear migration and the selection of neurogenic cell divisions during vertebrate retinogenesis. *J. Neurosci.* **27**, 10143-10152.
Berg, H. C. (1993). *Random Walks in Biology*. Princeton, NJ: Princeton University Press.
Calegari, F. and Huttner, W. B. (2003). An inhibition of cyclin-dependent kinases that lengthens, but does not arrest, neuroepithelial cell cycle induces premature neurogenesis. *J. Cell Sci.* **116**, 4947-4955.
Fish, J. L., Dehay, C., Kennedy, H. and Huttner, W. B. (2008). Making bigger brains – the evolution of neural-progenitor-cell division. *J. Cell Sci.* **121**, 2783-2793.
Harris, W. A. and Hartenstein, V. (1991). Neuronal determination without cell division in Xenopus embryos. *Neuron* **6**, 499-515.
Kimmel, C. B., Ballard, W. W., Kimmel, S. R., Ullmann, B. and Schilling, T. F. (1995). Stages of embryonic development of the zebrafish. *Dev. Dyn.* **203**, 253-310.
Kosodo, Y., Suetsugu, T., Suda, M., Mimori-Kiyosue, Y., Toida, K., Baba, S. A., Kimura, A. and Matsuzaki, F. (2011). Regulation of interkinetic nuclear migration by cell cycle-coupled active and passive mechanisms in the developing brain. *EMBO J.* **30**, 1690-1704.
Kusumi, A., Sako, Y. and Yamamoto, M. (1993). Confined lateral diffusion of membrane receptors as studied by single particle tracking (nanovid microscopy). Effects of calcium-induced differentiation in cultured epithelial cells. *Biophys. J.* **65**, 2021-2040.
Lange, C., Huttner, W. B. and Calegari, F. (2009). Cdk4/cyclinD1 overexpression in neural stem cells shortens G1, delays neurogenesis, and promotes the generation and expansion of basal progenitors. *Cell Stem Cell* **5**, 320-331.
Leonhardt, H., Rahn, H. P., Weinzierl, P., Sporbert, A., Cremer, T., Zink, D. and Cardoso, M. C. (2000). Dynamics of DNA replication factories in living cells. *J. Cell Biol.* **149**, 271-280.
Menozzi, F. D., Hanotte, O. and Miller, A. O. (1985). Stimulation of protein accumulation in HeLa cells by inhibitors of DNA replication. Ferritin. *FEBS Lett.* **193**, 49-53.
Meyer, E. J., Ikmi, A. and Gibson, M. C. (2011). Interkinetic nuclear migration is a broadly conserved feature of cell division in pseudostratified epithelia. *Curr. Biol.* **21**, 485-491.
Miyata, T. (2008). Development of three-dimensional architecture of the neuroepithelium: role of pseudostratification and cellular 'community'. *Dev. Growth Differ.* **50** (Suppl. 1), S105-S112.
Murciano, A., Zamora, J., Lopez-Sanchez, J. and Frade, J. M. (2002). Interkinetic nuclear movement may provide spatial clues to the regulation of neurogenesis. *Mol. Cell. Neurosci.* **21**, 285-300.
Norden, C., Young, S., Link, B. A. and Harris, W. A. (2009). Actomyosin is the main driver of interkinetic nuclear migration in the retina. *Cell* **138**, 1195-1208.
Pilaz, L. J., Patti, D., Marcy, G., Ollier, E., Pfister, S., Douglas, R. J., Betizeau, M., Gautier, E., Cortay, V., Doerflinger, N. et al. (2009). Forced G1-phase reduction alters mode of division, neuron number, and laminar phenotype in the cerebral cortex. *Proc. Natl. Acad. Sci. USA* **106**, 21924-21929.
Sauer, F. C. (1935). Mitosis in the neural tube. *J. Comp. Neurol.* **62**, 377-405.
Schenk, J., Wilsch-Brauninger, M., Calegari, F. and Huttner, W. B. (2009). Myosin II is required for interkinetic nuclear migration of neural progenitors. *Proc. Natl. Acad. Sci. USA* **106**, 16487-16492.
Takahashi, T., Nowakowski, R. S. and Caviness, V. S., Jr (1995). The cell cycle of the pseudostratified ventricular epithelium of the embryonic murine cerebral wall. *J. Neurosci.* **15**, 6046-6057.
Tsai, J. W., Lian, W. N., Kemal, S., Kriegstein, A. R. and Vallee, R. B. (2010). Kinesin 3 and cytoplasmic dynein mediate interkinetic nuclear migration in neural stem cells. *Nat. Neurosci.* **13**, 1463-1471.
Ueno, M., Katayama, K., Yamauchi, H., Nakayama, H. and Doi, K. (2006). Cell cycle progression is required for nuclear migration of neural progenitor cells. *Brain Res.* **1088**, 57-67.
Vassilev, L. T., Tovar, C., Chen, S., Knezevic, D., Zhao, X., Sun, H., Heimbrook, D. C. and Chen, L. (2006). Selective small-molecule inhibitor reveals critical mitotic functions of human CDK1. *Proc. Natl. Acad. Sci. USA* **103**, 10660-10665.
Zolessi, F. R., Poggi, L., Wilkinson, C. J., Chien, C. B. and Harris, W. A. (2006). Polarization and orientation of retinal ganglion cells in vivo. *Neural Dev.* **1**, 2.